Silver Nanoparticles, stabilized by *Tetrapleura tetraptera* from food waste, influence of extract on Nanoparticles' Surface Morphology and Antimicrobial properties

Vitus A. Apalangya[1*], Enock Dankyi[2], Jerry J. Harrison[2], Leticia Donkor[1], Samuel Darko[3], Angela Parry-Hanson Kunadu[4], Nicole S. Affrifah[1], and Abu Yaya[5]

[1]Department of Food Process Engineering, University of Ghana, Legon, Ghana
[2]Department of Chemistry, University of Ghana, Legon, Ghana
[3]School of Arts and Sciences, Florida Memorial University, USA
[4]Department of Nutrition and Food Science, University of Ghana, Legon, Ghana
[5]Department of Materials Science and Engineering, University of Ghana, Legon, Ghana

***Corresponding author:** vapalangya@ug.edu.gh

ABSTRACT

Plant extracts provide a sustainable and eco-friendly route to forming silver (Ag) nanoparticles (NPs). Synthesizing stabilized and monodisperse Ag NPs using plant extracts is challenging as several and various polyhydroxy compounds of extracts produce non-uniform dispersed NPs. In this study, stabilized Ag NPs were biosynthesized from environmentally friendly, non-toxic, novel aqueous *Tetrapleura tetraptera* fruit extract. The role of synthetic conditions like concentration of silver nitrate and pH were also investigated. Phytochemical and FT-IR analyses revealed that the extract contained polyphenols, flavonoids, and other polyhydroxy compounds. UV-Vis spectra indicated a surface plasmon resonance band at 420 nm typical of Ag NPs, and together with X-ray diffraction (XRD), X-ray photoelectron spectroscopy (XPS), and Energy Dispersive Spectroscopy (EDS), the patterns confirmed the formation of Ag NPs. The UV-Vis spectra and TEM micrographs showed that smaller, homogeneous, stabilized Ag NPs had an average particle size of 50 – 120 nm and 65 – 240nm (beyond 120nm is out of the range of nanoparticles). The *Tetrapleura tetraptera* extract made using 2.5 mM of $AgNO_3$ at a pH of 11.5 exhibited superior antibacterial properties depicted by enhanced growth inhibition and significantly lower ($P<0.05$). The minimum inhibition concentration (MIC) was determined against gram-negative and positive bacteria relative to the synthesized NPs at different pHs. The studies demonstrated the potential of deploring *Tetrapleura tetraptera* extract stabilized Ag NPs as potential antimicrobial agents in packaging and biomedical applications.

Keywords: *Tetrapleura tetraptera* fruit extract, green synthesis, silver nanoparticles, antibacterial properties, biomedical applications

1.0 INTRODUCTION

Beyond their enduring and aesthetic appeal, the great novel applications of noble metal nanoparticles (NPs), Such as gold (Au) and silver (Ag), in medicine, sensing, electronics, food, water, and

catalysis have been reported since antiquity [1-11]. Among metal nanoparticles, Ag and its nanoscale forms, for millennia, have been used to treat and disinfect bacterial infections due to their broad-spectrum biocidal effect towards a wide range of bacteria strains implicated in routine industrial and domestic processes[12, 13]. However, the behavior of Ag NPs as effective antimicrobial agents depends on their composition, shapes, and sizes [14-16]. Raza *et al.* noticed that smaller, spherical-shaped Ag NPs exhibited better antibacterial effects than triangular and larger spherical-shaped Ag NPs against gram-positive and negative bacteria strains [17]. However, due to their small size and high reactivity, uncapped metal nanoparticles are inclined to recombine, forming undesirable bulk forms, and reducing their activity. Ag NPs, due to their large surface-area-to-volume ratio, provide better contact with bacteria than bulk forms [16].

Solution-based methodologies have therefore been used to effectively stabilize and control shapes and sizes of Ag NPs, albeit requiring the use of expensive and potentially environmentally hazardous chemicals such as thiols, amines, polyols and acids due to their high reactivity [18-22]. Plant extracts have been proposed as environmentally safe alternatives as they contain diverse moderately reactive polyhydroxy compounds capable of reducing and capping Ag NPs [13, 23-25]. Extracts are biocompatible, and their usage produces Ag NPs with bioactive properties suitable for biological applications [26-28]. Moreover, the variety of polyhydroxy compounds in plant extracts could act cooperatively to confer suitable shapes, which may be challenging to obtain with single surfactant systems [29]. However, diverse polyhydroxy compounds in plant extracts lead to nanoparticle mixtures with varying sizes, shapes, and wide dispersity, diminishing their antibacterial activity. Narrowing down the spectrum of phytochemicals in the plant extracts through purification could present fewer suitable active compounds that come with increased process cost. Since NPs nucleation and stabilization are not only affected by stabilizers, choosing relevant plant extracts, and using appropriate experimental conditions could lead to stabilized and monodispersed colloidal NPs with desirable shapes and sizes. Recently, novel plant extracts and optimized conditions have been developed to obtain stabilized and well-dispersed green Ag NPs.

Tetrapleura tetraptera, locally known as "prekese" in Ghana, is a tropical flowering plant. Its fruits are consumed as food due to its pleasant aroma, appealing color , carbohydrate and protein content, and as medicine due to their abundant polyphenols, flavonoids, carotenoid, lactic acid and vitamin C contents [30, 31]. The fruit, root, and stem extract of this plant have been used and documented as food, and as traditional medicine in tropical African customs for managing a host of ailments including inflamaion, hypertension, epilepsy, diabetes mellitus, and arthritis; however, no study exploits the great phytochemical content of this plant extract for

the biosynthesis of bioactive metal NPs including Ag [32]. The study hypothesized that *Tetrapleura tetraptera* aqueous fruit extract can reduce and stabilize Ag NPs due to its great phytochemical content. The physicochemical characteristics of the synthesized Ag NPs under various experimental conditions were investigated using crystallographic, spectroscopic and microstructural techniques. In addition, the antimicrobial activities of the as-synthesized Ag NPs obtained at different pH and $AgNO_3$ concentrations were investigated against common gram-positive and negative bacterial food contaminants.

2.1. MATERIALS AND METHODS

All analytical chemicals were purchased from their respective sources and used without further purification. Silver nitrate ($AgNO_3$, 99.9%), sodium hydroxide (NaOH, 97%), hydrochloric acid (HCl, 37%) were purchased from Sigma Aldrich.

2.1. Preparation of *Tetrapleura tetraptera*

Fresh *Tetrapleura tetraptera* fruits were obtained from the Madina market and transported to the laboratory. They were cut into smaller pieces, washed thoroughly with tap water, rinsed with deionized water, and air-dried for two weeks. For easy and effective grinding, the air-dried samples were dried in an oven at 60 ^{o}C overnight to ensure complete dehydration. Next, the cut dried samples were milled for 1 hour using an attrition mill (Retsch, Rheinische StraBe 36.D-42781, Haan Germany). The samples were sieved using a sieve shaker with stainless steel sieves stacked from coarse to fine mesh (80, 60, 20 µm). Subsequently, 10 g of the milled powdered samples was mixed thoroughly in 25 ml ethanol and water solution (2:1 v/v). The resulting mixture was boiled at 60 ℃ for 30 minutes under constant stirring to obtain highly viscous extracts and subsequently kept at room temperature to cool. The cooled mixture was filtered using a Whatman No.1 filter paper to get a clearer solution of the extract. The extracts were then stored in a refrigerator until further use.

2.2. Phytochemical screening of extracts

The phytochemical content of the plant extracts was analyzed according to the method adopted by Bashair *et al.* [33]. The availability of phytochemicals such as polyphenols, flavonoids, saponins and tannins in the *Tetrapleura sp* extracts were determined. The detailed procedure for analyzing each phytochemical is shown in the supplementary information (section 1)

2.3. Synthesis of Silver Nanoparticles

All reagents used were of analytical grade. Ag nitrate ($AgNO_3$) solution was prepared by dissolving an appropriate amount of $AgNO_3$ salt in 100 mL deionized water to obtain approximately 0.1 M stock solution. The following reactions were performed to determine the effect of AgNO3 concentration on the properties of the Ag NPs. Aliquots of the stock solution were pipetted and added dropwise to Erlenmeyer flasks containing 25 ml diluted *Tetrapleura tetraptera* fruit extract, which was composed of 5 ml of plant extract and varying amounts of deionized water, to obtain a prepared final reaction solution containing 25-, 50- and 100-mM concentrations of $AgNO_3$. To evaluate the effect of pH on the properties of the Ag NPs during synthesis, the reaction was performed at three different pH values (4.2, 7.4 and 11.2) using final $AgNO_3$ concentrations of 25, 50 and 100 mM. The effect of changing concentration of $AgNO_3$ salt and pH during the synthesis was monitored and analyzed using UV-Vis spectroscopy and TEM analyses.

2.4. Characterization of Biosynthesized Colloidal Silver Nanoparticles

2.4.1. UV-Vis Spectroscopy

The UV-Vis absorption patterns were obtained and analyzed using a Shimadzu UV-3600 UV-Vis-NIR spectrophotometer. The effect of $AgNO_3$ concentration on the UV-Vis spectra of the colloidal Ag NPs synthesized was investigated at three different concentrations of $AgNO_3$ (2.5, 50 and 100 mM). In addition, the influence of pH (at 4.2, 7.4 and 11.2) on the UV-Vis spectra of the Ag NPs was also studied using two concentrations of $AgNO_3$ (25 and 100 mM).

2.4.2. Fourier transform infra-red spectroscopy, X-Ray Diffraction and X-ray photoelectron spectroscopy

The Fourier transform infra-red Spectroscopy (FTIR) patterns were measured and recorded using a PerkinElmer Spectrum 100 spectrophotometer. X-Ray Diffraction (XRD) analyses were performed using Rigaku DMAX 2100 diffractometer (Rigaku, Tokyo, Japan) with monochromatic CuK α radiation ($\lambda = 0.154056$ nm) at 40 kV and 30 mA. The surface chemistry and elemental composition of the colloidal Ag NPs were studied using X-ray photoelectron spectroscopy (XPS) measurements. A load-locked Kratos XSAM 800 surface analysis system was used to acquire the XPS spectra.

2.4.3. Transmission Electron Microscopy

The surface morphological analysis of the biosynthesized colloidal Ag NPs was conducted using high-resolution transmission electron microscopy (H-8000 TEM microscope). In a sonication bath, the colloidal samples were prepared by sonicating 5 ml of the biosynthesized Ag NPs for 5 minutes. A drop of the colloidal Ag NPs solution

made from two concentrations of $AgNO_3$ (2.5 and 100 mM) at pH of 11.2 was deposited on a carbon grid (carbon-coated copper grid and the excess solution was removed using tissue paper) and enough time was allowed for drying of prepared sample grids at room temperature.

2.5. Antimicrobial assays

2.5.1. *In vitro* antimicrobial assay

S. Typhimurium was used in this study. Each stock bacteria species was sub-cultured on a Mueller-Hinton agar (Park Scientific Limited) plate and incubated overnight at 37ºC to obtain pure cultures. About 3-4 single colonies from the bacteria plate were selected, inoculated into Mueller-Hinton broth and incubated at 37 ºC overnight, for the bacteria to reach the log phase of growth. The log phase bacteria were diluted with sterile saline to achieve a turbidity of 0.5 McFarland standard, an approximate concentration of 2 x 10^8 CFU/ml.

Log phase bacteria at a concentration range of 1 x10^2 to 1x10^7 CFU/ml were incubated with different concentrations of the test agents (0 % -100 %) and 10% Alamar Blue® reagent at 37ºC for 6-8 hrs. Absorbance was read at 540 nm, reference 595 nm, using a spectrophotometer (TECAN Sunrise Wako). In determining the bactericidal and bacteriostatic properties of concentrations of the Ag NPs (6 – 60 µg/mL) and 10 % Alamar Blue®. The reducing power of cells to convert the Alamar Blue component resazurin to the pink resorufin was used to determine the Minimum Inhibitory Concentration (MIC) of the samples. The least concentration of compounds with no observable color change was noted as the MIC.

3.0 RESULTS AND DISCUSSION

3.1. Phytochemical Analysis

The phytochemical analysis indicated that the aqueous *Tetrapleura tetraptera* fruit extract contained polyphenols, saponins, glycosides, tannins, and flavonoids as shown in Table 1which constituent with reported study.

Table 1: Phytochemical analysis of aqueous *Tetrapleura tetraptera* fruit extract

Name of test	Phytochemicals	Tetrapleura
Ferric chloride test	Polyphenols	+
Alkaline reagent test	Flavonoids	+
Braymer's test	Tannins	+
Foam test	Saponins	+
Salkowki's test	Terpenoids	-
Keller killiani test	Glycosides	+

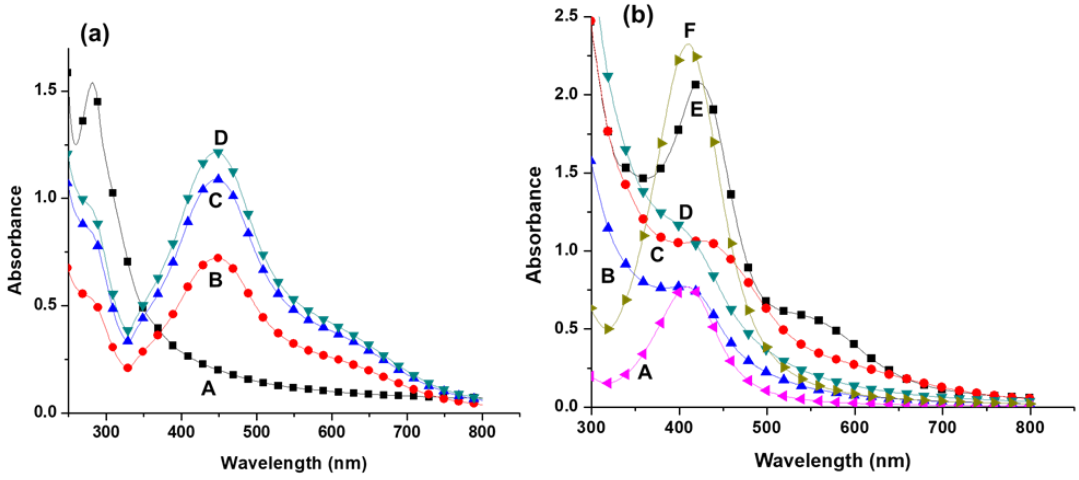

Figure 1. UV-Vis patterns (a) A: pure *Tetrapleura terapleura* extract (TTE), B: Ag NPs 25 nM $AgNO_3$, C: 50 mM $AgNO_3$ D: 100 mM $AgNO_3$ (b) Ag NPs synthesized at A: pH 7.4 & 25 mM $AgNO_3$, B: pH 7.4 & 100 mM $AgNO_3$, C: pH 4.2 & 100 mM $AgNO_3$, D: pH 4.2 & 25 mM $AgNO_3$, E: pH 11.2 & 100 mM $AgNO_3$ and F: pH 11.2 and 25 mM $AgNO_3$

3.2. UV-Vis spectroscopy analysis

The bioreduction of Ag^+ ions to Ag (Ag^0) nanoparticles were observed by monitoring the distinct color changes and the appearance of a typical Ag surface plasmon resonance (SPR) band in UV–Vis spectroscopy measurements accompanying the reactions. The biosynthesis proceeded with distinct change of the solution color from pale brown to dark brown as depicted in the supplementary information (section 2). The appearance of a characteristic SPR band at 420 nm and together with microstructural studies confirmed the formation of Ag NPs (figure 1).

3.3. FT-IR, XRD and XPS Analysis

FT-IR studies were performed to confirm the presence of polyphenolic phytochemicals in the *Tetrapleura tetraptera* fruit extract and as well as on the surface of biosynthesized colloidal Ag NPs. Fig. 2(a)A and fig. 2(a)B depict the FT-IR patterns of pure fruit extract and biosynthesized Ag NPs respectively. Both exhibited similar molecular vibrational patterns. However, the patterns showed strong sharp band at 3320 cm^{-1} which is typical of -OH stretching vibration associated with polyols which can be related to the polyphenols and other polyhydroxy phytochemicals present in the extract. A relatively more robust band around 2912 cm^{-1} and a weak shoulder at about 2800 cm^{-1} are characteristic symmetric and asymmetric stretching vibrations of CH respectively of an aliphatic hydrocarbon attributable to the polysaccharide or terpenoid phytochemicals present in the fruit extract. The band around 1635 cm^{-1} is the bending vibrational mode typical of water in the extract as well as in the colloidal Ag NPs. Finally, the band at 1087 cm^{-1} can be related to the C-O-C stretching vibration of the CH_2OH group on a polysaccharide compound in the extract [37]. These observations are consistent with earlier study that plant extracts possess suitable functional groups which capped the surface of the Ag NPs stabilizing them as stable colloidal solutions [38].

X-ray diffraction (X-RD) pattern of the biosynthesized colloidal Ag NPs is depicted in Fig. 2 (b). Typical of Ag NPs, four characteristic peaks are indexed at 2θ = 38.1°, 44.2°, 64.4°and 77.3° and correspond to the following Bradley crystal faces of (1 1 1), (2 0 0), (2 2 0) and (3 1 1) of Ag with JCPDS card (file No JCPDS # 04-0783). The surface chemical composition of the biosynthesized Ag NPs is depicted by XPS patterns in the Fig. 2 (c) and (d) showing the structure and the chemical identity of the species involved. It is evident that the as-synthesized sample is composed of carbon (C), oxygen (O_2) and Ag with no other chemical or elemental impurities. There is a doublet with binding energies at about 363 and 379 eV which can be associated with Ag3d3/2 and Ag3d5/2 characteristic of Ag. The intensity ratio of this doublet peak is 2:1 and is consistent with similar literature report (6).

The elemental composition of Ag on the surface of the sample is 17.7%, relative to the other elements in the synthesized sample. This lower percentage composition relative to the amount quantified by the EDS may be due to the lower depth of measurement of the XPS technique [6].

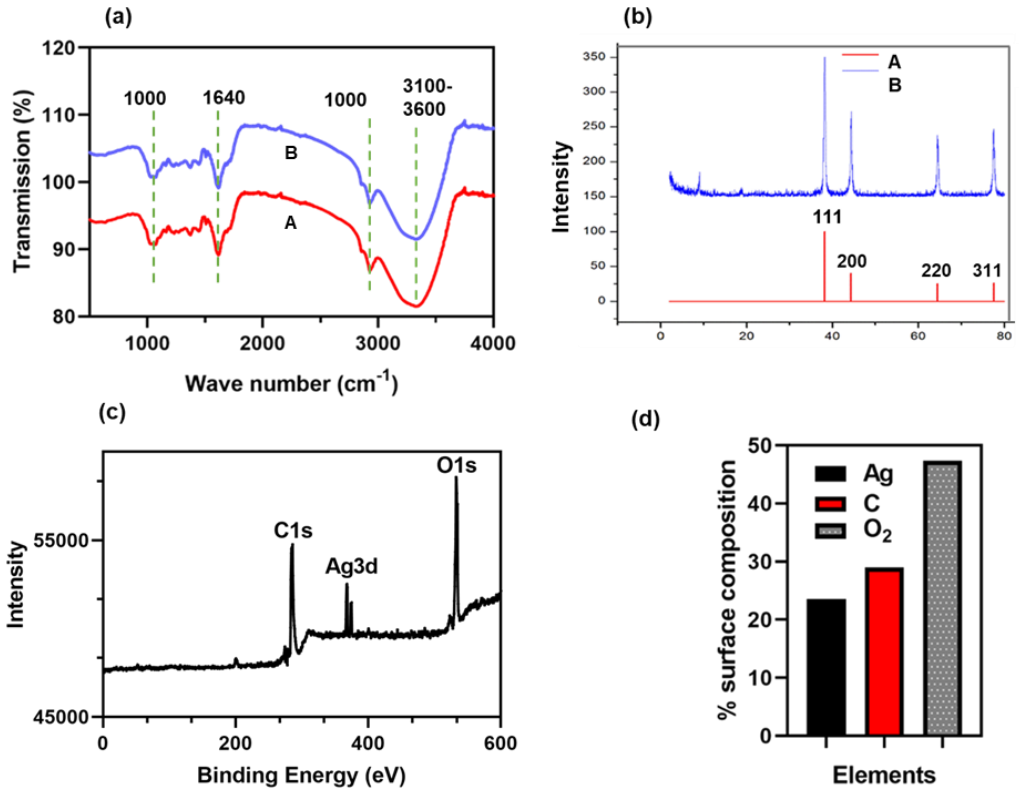

Figure 2. (a) FT-IR patterns of A: Tetrapleura tetraptera fruit extract and B: synthesized Ag NPs (b) XRD pattern of synthesized Tetrapleura tetraptera fruit extract stabilized Ag NPs (c) XPS pattern of *Tetrapleura tetraptera* fruit extract stabilized Ag NPs (d) percentage elemental composition from XPS studies.

3.4. Scanning Electron Microscope and EDX Analysis

The surface morphology of Ag NPs which were synthesized at a pH of 11.2 was acquired and analyzed by FETEM and EDX, as depicted in fig.3. The nanoparticles exhibited uniform morphology with spherical shapes and an average size of 60 nm (fig. 4(b)). NPs appeared well dispersed with little agglomeration. The NPs were well stabilized on the surface of the fruit extract phytochemicals which likely played a role in minimizing particle to particle interaction resulting in reduced particle combination. Moreover, the abundance of polyphenols, flavonoids and polysaccharides in the extract likely adsorbed onto the surface of the nanoparticles. This phenomenon has the tendency to significantly reduce the surface energy of the particles minimizing their reactivity in the process thereby preventing particle agglomeration.

Finally, the significant reduction of $AgNO_3$ concentration drastically shortens the time for the concurrent formation and growth of the Ag NPs with the benefit of promoting the production of monodispersed Ag NPs with less particle recombining. As shown in fig. 4(c), there is a 3keV intense spectral peak which is indicative of the formation of Ag NPs as shown in the EDX pattern. Fig. 3(b) is a depiction of the surface morphology of Ag NPs synthesized at a pH of 11.2 using 100 mM $AgNO_3$ concentration. It is evident that there is a wide particle size variation ranging from 70 – 240 nm. The particle shapes vary from spherical to other complicated morphologies. The particles appeared to be coalescing. Compared to the particles formed at the same pH of 11.2 but at 2.5 mM $AgNO_3$ concentration, it can be observed that more nanoparticles are formed for the same amount of plant extract with reduced mono-dispersity. The agglomeration of the NPs is a result of insufficient stabilizing agents. Mono-dispersity of the NPs can be attained by having particles surfaces well stabilized immediately they are formed. This will minimize undesirable particle interactions reducing nucleation outpacing particle growth. It is therefore prudent to increase the amount of plant extract to provide more stabilizing agents.

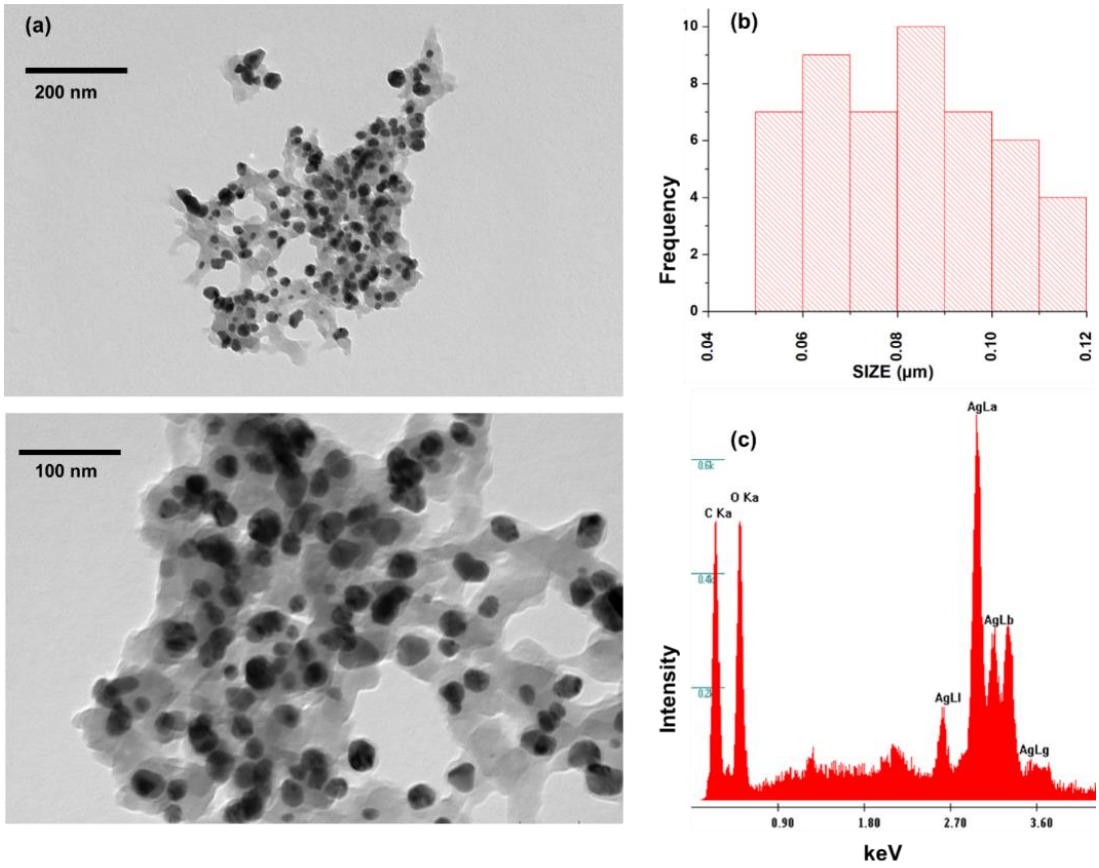

Figure 3. (a) Low and high magnification TEM image of Ag NPs synthesized from 2.5 mM of $AgNO_3$ at pH of 11.2 (b) average size of Ag NPs (c) EDX pattern of Ag NPs

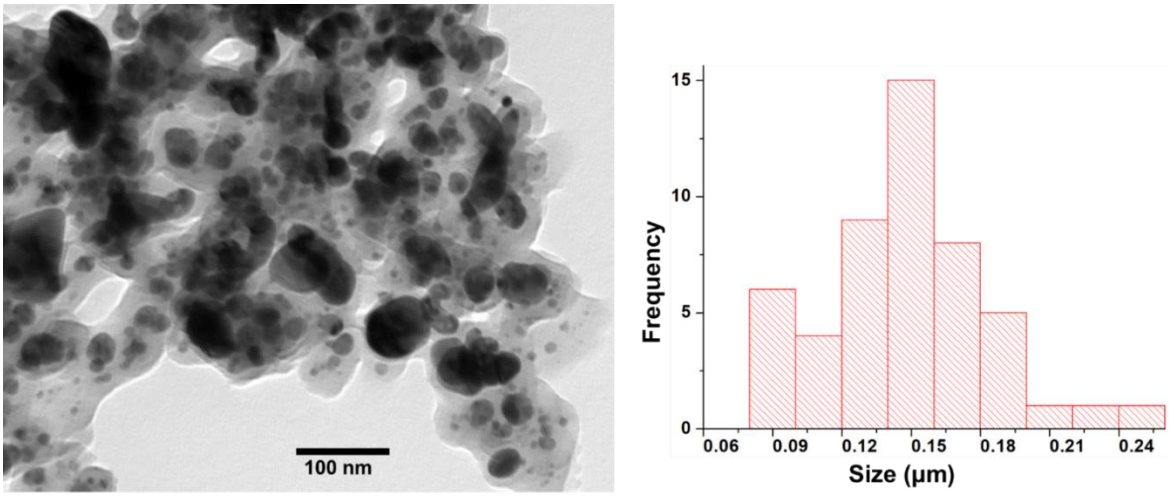

Figure 4: (a) TEM image of Ag NPs at 100 mM of $AgNO_3$ at pH of 11.2 (b) average size of Ag NPs

3.5. Mechanism of formation and stabilization of Silver Nanoparticles

Most plant extracts are weak or moderate reducing agents compared to stronger synthetic oxidizing agents such as sodium borohydride, sodium dodecyl sulfate, and poly (vinyl pyrolidone) [39, 40]. As a result, their rate of reduction of Ag ions to Ag NPs is slow, this inadvertently enables concurrent nucleation and growth of metal nanoparticles. The new and old nuclei readily recombine due to their high surface energy and closeness in space and time, therefore yielding polydisperse NPs. To overcome polydispersity, metal NPs are synthesized at high temperatures. Even

though reducing Ag^+ ions to Ag NPs at elevated temperatures produces considerable high monodisperse NPs, in most instances, the NPs produced have broad size distribution with a variety of nanoparticle geometry. In this study, the effect of polyphenolic, flavonoid and polysaccharide laden *Tetrapleura tetraptera* fruit extract mediated the reduction of Ag^+ ions to Ag NPs. Flavonoids and polyphenolic compounds have been established to be effective reducing and stabilizing agents whereas polysaccharides due to their long polymer chains can effectively stabilize the whole body of NPs in solution. At high pH (11.2), enol forms of flavonoids and phenolic compounds are capable of releasing electrons that can interact with Ag^+ ions reducing them to Ag NPs as shown in fig, 5. Basic synthetic medium can result in the activation of the flavonoids and polyphenolic compounds making them better reducing agents. Relative to their neutral or moderately acidic pH media counterparts as shown as depicted in figure 5.

3.6. Antibacterial Analysis

The minimum inhibition concentration (MIC) determined for each bacteria species treated with the prepared Ag NPs at different pH are shown in figure 6. To evaluate the difference in bacterial growth inhibition among the different Ag NPs biosynthesized using different combinations of AgNO3 concentrations and pH, a triplicated minimum inhibition concentration (MIC) of each class of Ag NPs was evaluated versus the three strains of bacteria – Salmonella Typhimurium (fig 6).

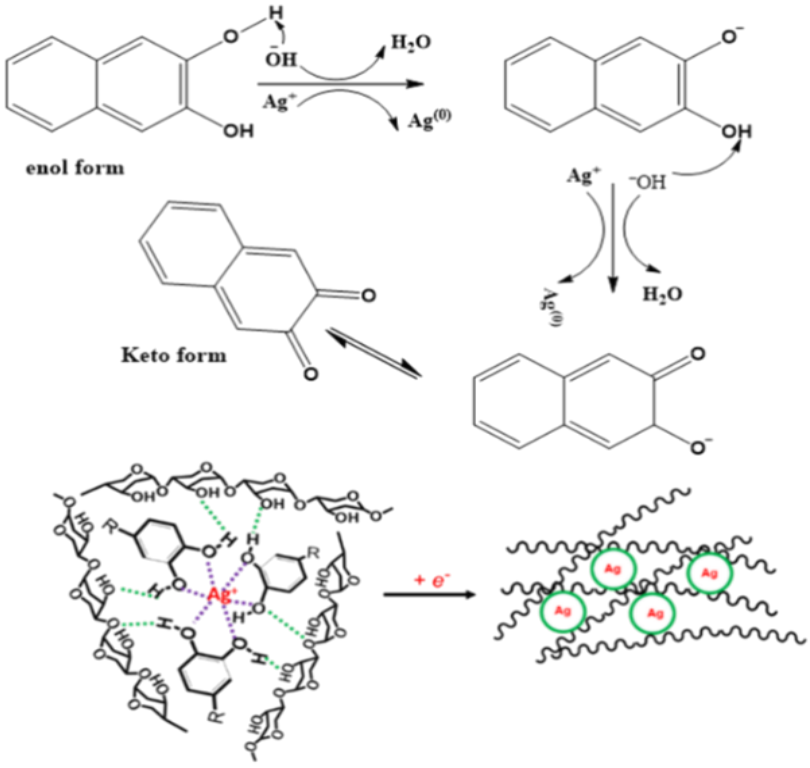

Figure 5. A schematic showing the interaction of Ag ions before and after reduction into colloidal silver nanoparticles with phytochemicals.

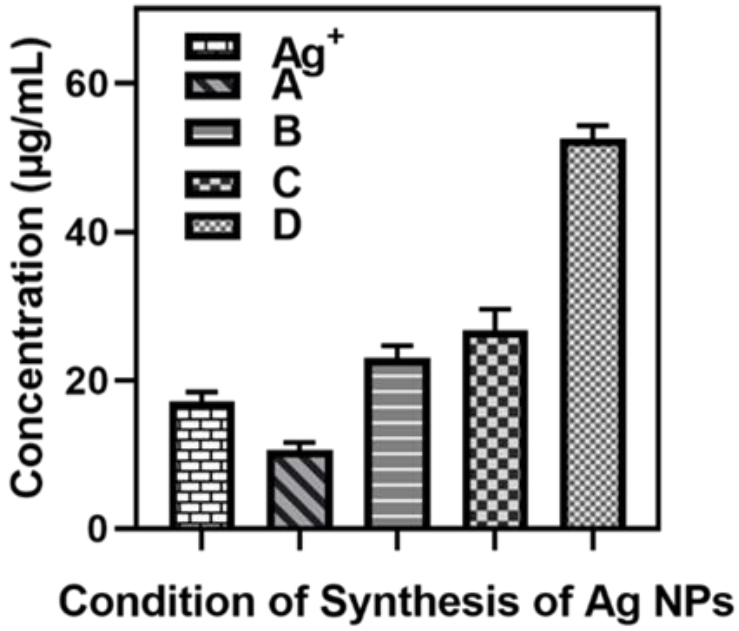

Figure 6. The least concentration (MIC) of Ag NPs needed to inhibit visible growth of *Salmonella typhimurium* with each bacteria treated Ag^+, and Ag NPs synthesized using a combination of the following $AgNO_3$ concentration and pH: A; 25 mM and11.2, B; 100 mM and11.2, C; 25 mM and 7.4, and D: 25 mM and 4.7 respectively

It is evident from this MIC study that *Tetrapleura tetraptera* fruit caped Ag NPs made using $AgNO_3$ with 2.5 mM at a pH of 11.2 (fig. 6 A) exhibited significantly ($P<0.05$) the lowest MIC values compared to the other *Tetrapleura tetraptera* caped Ag NPs at different $AgNO_3$ concentrations and pH combinations (fig. 6 B, C, D and Ag+ or $AgNO_3$). Generally Ag NPs made in neutral and basic media also exhibited significantly ($P<0.05$) lower MIC values compared to NPs made in acidic medium. However, there was an insignificant difference in MIC values for Ag NPs synthesized at a pH of 11.2 with $AgNO_3$ concentration of 100 mM and 7.4 with $AgNO_3$ concentration of 2.5 mM. This clearly showed that a combination of both basic pH and low $AgNO_3$ concentration is necessary for producing Ag NPs with the most active antibacterial properties. It is evident that Ag NPs synthesized at acidic pH (3.6) exhibited the lowest antibacterial activity. Noticeably, the efficacy of the Ag NPs strongly depended on the concentration of the reagent $AgNO_3$ and the reacting pH which is also directly related to

and the reacting pH which is also directly related to the size of the NPs as smaller size Ag NPs exhibited better antibacterial activity compared to bigger size NPs. As shown by the SEM micrographs, Ag NPs synthesized using 100 mM agglomerates forming larger particles thereby losing their size associated large surface area to volume ratio reactivity. The ease of reduction of Ag^+ ions to Ag NPs depends on the degree of dissociation of polyphenols and the resulting release of electrons and stabilization of the Ag NPs by the enolates. Since at basic pH (11), the dissociation of the polyphenols occurs more readily and than at acidic pH (3.6), more Ag NPs will be produced and stabilized per unit volume of colloidal solution for a given $AgNO_3$ concentration in the basic medium than in acidic medium. Mechanistically, Ag NPs inhibit bacteria growth through attachment to the surface of bacteria cells and the resulting penetration of the cell wall or release of ions and reactive oxygen species which are all favoring smaller size NPs compare to larger size ones in this study [41].

4.0 CONCLUSION

In this study, aqueous *Tetrapleura tetraptera* fruit extract has been used for the first time as a green reducing and stabilizing agent in synthesizing eco-friendly Ag NPs. Phytochemical analysis and FT-IR studies showed that the extract contains several polyhydroxy compounds with potential reducingand stabilizing capacity. The formation of the Ag NPs was characterized and confirmed using UV-Visible, XRD, and XPS spectra. The size and effective stabilization of the NPs are dependent on the concentration of the $AgNO_3$ and the pH of the reaction medium. Lower concentration $AgNO_3$ and basic medium produced smaller size, well dispersed and stabilized Ag NPs whereas higher $AgNO_3$ and acidic medium resulted in larger size NPs, varying size and shapes, and agglomerated Ag NPs. The biosynthesized NPs exhibited broad antibacterial properties by inhibiting the growth of both gram-positive gram-negative *Salmonella Typhimurium.* Ag NPs which were synthesized using lower concentration of Ag NPs and in basic medium were the most efficacious as the Ag NPs exhibited better antibacterial properties with the lowest MIC values against gram-negative bacteria. Conceivably, these biosynthesized Ag NPs can be incorporated into packaging systems and biomedical membranes for food and wound healing applications.

DECLARATION OF COMPETING INTEREST

The authors confirm that there are no known conflicts of interest associated with this publication and there has been no significant financial support for this work that could have influenced its outcome.

ACKNOWLEDGEMENT

Authors are grateful to the University of Ghana Building a New Generation of African Academics (BANGA-AFRICA) Project funded by the Carnegie Corporation of New York for financial support. We are grateful to The Electron Microscopy Center at the University of South Carolina for their assistance with our TEM analysis.

DATA AVAILABILITY

The data used to support the findings of this research are included within the article.

REFERENCES

[1] G.G. de Lima, D.W. de Lima, M.J. de Oliveira, A.B. Lugão, M.T. Alcântara, D.M. Devine, M.J. de Sá, ACS Applied Bio Materials 1 (2018) 1842.

[2] Y. Ran, P. Strobbia, V. Cupil-Garcia, T. Vo-Dinh, Sensors and Actuators B: Chemical 287 (2019) 95.

[3] N. Karim, S. Afroj, S. Tan, K.S. Novoselov, S.G. Yeates, Scientific reports 9 (2019) 8035.

[4] M. Park, J. Im, M. Shin, Y. Min, J. Park, H. Cho, S. Park, M.-B. Shim, S. Jeon, D.-Y. Chung, Nature nanotechnology 7 (2012) 803.

[5] A. Martínez-Abad, J.M. Lagaron, M.J. Ocio, Journal of agricultural and food chemistry 60 (2012) 5350.

[6] V. Apalangya, V. Rangari, B. Tiimob, S. Jeelani, T. Samuel, Applied Surface Science 295 (2014) 108.

[7] R. Bryaskova, N. Georgieva, D. Pencheva, Z. Todorova, N. Lazarova, T. Kantardjiev, Colloids and Surfaces A: Physicochemical and Engineering Aspects 444 (2014) 114.

[8] P. Xu, C. Cen, N. Chen, H. Lin, Q. Wang, N. Xu, J. Tang, Z. Teng, Journal of colloid and interface science 526 (2018) 194.

[9] Z. Qiao, Y. Yao, S. Song, M. Yin, J. Luo, Journal of Materials Chemistry B 7 (2019) 830.

[10] w.A. Oddy, M. Bimson, S.L. Niece, Studies in Conservation 28 (1983) 29.

[11] R.E. Leader-Newby, Silver and society in late antiquity: functions and meanings of silver plate in the fourth to seventh centuries. Routledge, 2017.

[12] W. Hill, D. Pillsbury, Baltimore, 1939.

[13] M. Pollini, F. Paladini, M. Catalano, A. Taurino, A. Licciulli, A. Maffezzoli, A. Sannino, Journal of Materials Science: Materials in Medicine 22 (2011) 2005.

[14] A. Roy, O. Bulut, S. Some, A.K. Mandal, M.D. Yilmaz, RSC advances 9 (2019) 2673.

[15] O.V. Mikhailov, Crystallography Reviews 25 (2019) 54.

[16] J.R. Morones, J.L. Elechiguerra, A. Camacho, K. Holt, J.B. Kouri, J.T. Ramírez, M.J. Yacaman, Nanotechnology 16 (2005) 2346.

[17] M. Raza, Z. Kanwal, A. Rauf, A. Sabri, S. Riaz, S. Naseem, Nanomaterials 6 (2016) 74.

[18] S. Iravani, H. Korbekandi, S.V. Mirmohammadi, B. Zolfaghari, Research in pharmaceutical sciences 9 (2014) 385.

[19] Z. Chen, T. Balankura, K.A. Fichthorn, R.M. Rioux, ACS nano 13 (2019) 1849.

[20] J. Xiong, X.-d. Wu, Q.-j. Xue, Colloids and Surfaces A: Physicochemical and Engineering Aspects 423 (2013) 89.

[21] Y. Wang, J.F. Wong, X. Teng, X.Z. Lin, H. Yang, Nano Letters 3 (2003) 1555.

[22] H. Hu, X. Wu, H. Wang, H. Wang, J. Zhou, Carbohydrate Polymers 213 (2019) 419.

[23] G.M. Nazeruddin, N.R. Prasad, S.R. Prasad, Y.I. Shaikh, S.R. Waghmare, P. Adhyapak, Industrial Crops and Products 60 (2014) 212.

[24] R.D. Rivera-Rangel, M.P. González-Muñoz, M. Avila-Rodriguez, T.A. Razo-Lazcano, C. Solans, Colloids and Surfaces A: Physicochemical and Engineering Aspects 536 (2018) 60.

[25] K. Hileuskaya, A. Ladutska, V. Kulikouskaya, A. Kraskouski, G. Novik, I. Kozerozhets, A. Kozlovskiy, V. Agabekov, Colloids and Surfaces A: Physicochemical and Engineering Aspects (2019) 124141.

[26] M.K. Swamy, K. Sudipta, K. Jayanta, S. Balasubramanya, Applied nanoscience 5 (2015) 73.

[27] M.N. Nadagouda, N. Iyanna, J. Lalley, C. Han, D.D. Dionysiou, R.S. Varma, ACS Sustainable Chemistry & Engineering 2 (2014) 1717.

[28] M.F. Zayed, R.A. Mahfoze, S.M. El-kousy, E.A. Al-Ashkar, Colloids and Surfaces A: Physicochemical and Engineering Aspects (2019) 124167.

[29] S.S. Nogueira, A.R. de Araujo-Nobre, A.C. Mafud, M.A. Guimarães, M.M.M. Alves, A. Plácido, F.A.A. Carvalho, D.D.R. Arcanjo, Y. Mascarenhas, F.G. Costa, P. Albuquerque, P. Eaton, J.R. de Souza de Almeida Leite, D.A. da Silva, V.S. Cardoso, International Journal of Biological Macromolecules 135 (2019) 808.

[30] B. Darfour, S. Agbenyegah, D. Ofosu, A. Okyere, I. Asare, Radiation Physics and Chemistry 102 (2014) 153.

[31] D.A. Abugri, G. Pritchett, Journal of herbs, spices & medicinal plants 19 (2013) 391.

[32] J.A. Ojewole, C.O. Adewunmi, Journal of Ethnopharmacology 95 (2004) 177.

[33] L.A.A. Bashair H Al Kinani, Der Pharma Chemica (2017).

[34] Y. Htwe, W. Chow, Y. Suda, M. Mariatti, Materials Today: Proceedings 17 (2019) 568.

[35] D. Paramelle, A. Sadovoy, S. Gorelik, P. Free, J. Hobley, D.G. Fernig, Analyst 139 (2014) 4855.

[36] S.M. Roopan, Rohit, G. Madhumitha, A.A. Rahuman, C. Kamaraj, A. Bharathi, T.V. Surendra, Industrial Crops and Products 43 (2013) 631.

[37] T. Petit, L. Puskar, T. Dolenko, S. Choudhury, E. Ritter, S. Burikov, K. Laptinskiy, Q. Brzustowski, U. Schade, H. Yuzawa, The Journal of Physical Chemistry C 121 (2017) 5185.

[38] S. Ramanathan, S.C.B. Gopinath, P. Anbu, T. Lakshmipriya, F.H. Kasim, C.-G. Lee, Journal of Molecular Structure 1160 (2018) 80.

[39] R. Das, M. Das, International Journal of Plastics Technology (2019) 1.

[40] L. Fontana, M. Bassetti, C. Battocchio, I. Venditti, I. Fratoddi, Colloids and Surfaces A: Physicochemical and Engineering Aspects 532 (2017) 282.

[41] E.T. Hwang, J.H. Lee, Y.J. Chae, Y.S. Kim, B.C. Kim, B.I. Sang, M.B. Gu, Small 4 (2008) 746.

.